Chemical Engineering Journal 153 (2009) 231–235

Contents lists available at ScienceDirect

Chemical Engineering Journal

journal homepage: www.elsevier.com/locate/cej

Short communication

Limiting flux prediction during tubular ultrafiltration

Abdellah Beicha [a,*], Radia Zaamouche [b]

[a] Jijel University, Faculty of Engineering, Department of Industrial Chemistry, PB. 98, Ouled Aissa, 1800 Jijel, Algeria
[b] Jijel University, Faculty of Engineering, Department of Mechanical Engineering, PB. 98, Ouled Aissa, 1800 Jijel, Algeria

ARTICLE INFO

Article history:
Received 17 February 2009
Received in revised form 6 June 2009
Accepted 10 June 2009

Keywords:
Ultrafiltration
Limiting flux
Polarized layer
Gel layer
Critical concentration

ABSTRACT

Ultrafiltration of polyethylene glycol aqueous solutions was analyzed using concentration polarization-gel layer model. The model is based on coupling concentration polarization layer and gel layer growth. The concentration polarization layer development is given by the convective-diffusion equation. However, the gel layer growth model is obtained by using the experimental observations. The limiting flux was found to be proportional to the square root of the axial velocity. Beyond the critical concentration, both concentration polarization and gel formation are the main factors controlling the limiting flux in the tubular UF system. The developed semi-empirical model, which contains a single empirical constant to be evaluated from experiments, predicted satisfactorily the limiting flux data over the range of experimental variables examined in this study.

1. Introduction

When a solution that contains macromolecules is forced through a membrane, the flux exhibits a linear dependence on pressure at very low pressure; however, as pressure increases the flux becomes independent of applied transmembrane pressure (TMP) [1–3]. This phenomenon is called limiting flux. As the limiting flux is the maximum attainable flux under the operating conditions, the prediction of the limiting flux is very important for operation design. Among the many models that have been developed to study the limiting phenomena, the one commonly used is the gel polarization model [4]. Gel polarization model assumes that at high TMP, the wall concentration of the solute reaches a maximum value, which indicates that a layer of "gel" has formed at the membrane surface, which induces an additional resistance to the permeate flow. Some of the other approaches include, the integral method model developed by Trettin and Doshi [5], a viscosity theory for the limiting flux developed by Aimar and Field [6].

Beicha et al. [7] developed a model which couples the formation of a gel layer on the membrane surface and the presences of a polarized layer above the gel. The model compared with experimental permeate fluxes obtained from the ultrafiltration of polyethylene glycol (PEG) using polyethersulphone membrane (4000 MWCO). The model gave an excellent prediction of the permeate fluxes for low and medium transmembrane pressures. However, for higher transmembrane pressures the model overpredicts the permeate fluxes. In this work, the same concept employed by Beicha et al. [7] and Sulaiman et al. [8] is used to predict limiting flux when the permeate flux becomes independent of pressure during tubular ultrafiltration.

2. Experimental

2.1. Experimental set-up

The schematic diagram of the experimental set-up is shown in Fig. 1. The process material from a 40 l feed tank is fed to the membrane unit via a pump (Gep Vertical Spco CDL F8). The pump has a maximum delivery capacity of 8 m^3/h. A strainer is fitted upstream of the feed pump to trap any particles larger than 250 μm that may be present in the feed stream.

A tubular membrane module (Model B1-ES625) encased in a stainless steel housing was obtained from PCI Membrane Systems Ltd. (United Kingdom). The system consists of 18 tubes connected in series by special cap ends, with each tube measuring 1.2 m in length and 1.25 cm inside diameter.

The permeate line is passed through valve V3 before being returned into the feed tank. Similarly, the retentate line is also recycled back into the feed tank. Permeate samples are collected in a glass cylinder placed on an electronic balance (Milliot, model F998-6) with direct interfacing to a computerized data acquisition software.

2.2. Materials

The materials used for the experiments were polyethylene glycol (PEG) of 20,000 MW and distilled water. The different solutions

Abbreviations: TMP, transmembrane pressure (bar); PEG, polyethylene glycol; MWCO, molecular weight cut-off.

* Corresponding author. Tel.: +213 71916914.
E-mail address: abeicha@yahoo.com (A. Beicha).

1385-8947/$ – see front matter © 2009 Elsevier B.V. All rights reserved.
doi:10.1016/j.cej.2009.06.018

Nomenclature

A	empirical constant ($m^{1/2}/s^{1/2}$)
C	concentration (wt.%)
C_b	bulk concentration (wt.%)
C_{cr}	critical bulk concentration (wt.%)
C_g	gel concentration (wt.%)
D	diffusivity (m^2/s)
d	inner membrane diameter (m)
l	thickness of gel layer
L	membrane length (m)
Δp	transmembrane pressure (bar)
$\tilde{R}_g$	specific gel resistance (bar s/m^2)
R_m	membrane resistance (bar s/m)
u_0	bulk velocity (m/s)
u_p	permeate flux (m/s)
u_{lim}	limiting flux (m/s)
u_z	axial velocity (m/s)
u_r	radial velocity (m/s)

Greek letters

ε	solidosity (%)
ε_b	bulk solidosity (%)
ε_g	solidosity of the gel layer (%)

were prepared by dissolving predetermined amount of the PEG in known volumes of distilled water. The concentrations of the solution (weight%) used in this study were in the range 0.1–1.5 wt.%. The membrane used is polyethersulphone (ES404) with molecular weight cut-off 4000 (PCI).

2.3. Experimental procedure

Solutions of polyethylene glycol (PEG) with an average molecular weight of 20,000 were used in all experiments. The feed material was prepared by dissolving predetermined amount of PEG in freshly distilled water. A typical run began by changing the feed material into the feed tank. The flow into the system was then adjusted to the required cross-flow velocity. Another variable, which must also be set is the transmembrane pressure (TMP) and this was accomplished by adjusting valves V1 and V2. The weight of permeate, collected as a function of time, was continuously monitored on the balance. Permeate flux was calculated by numerical differentiation of the permeate mass versus time and divided by the product density times the total area of the membrane system. At times, samples of retentate as well as permeate were collected and kept in vials for further analysis. In order to maintain a constant solute concentration in the reservoir, permeate collected on the balance was periodically returned to the reservoir. Freshly prepared feed material was used for each experiment using pre-cleaned membrane.

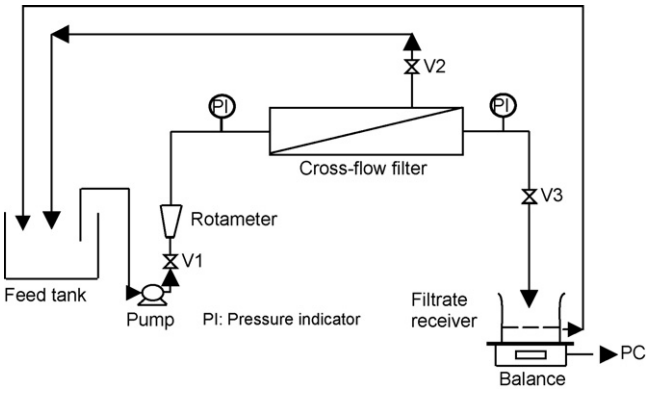

Fig. 1. Schematic diagram of the experimental set-up.

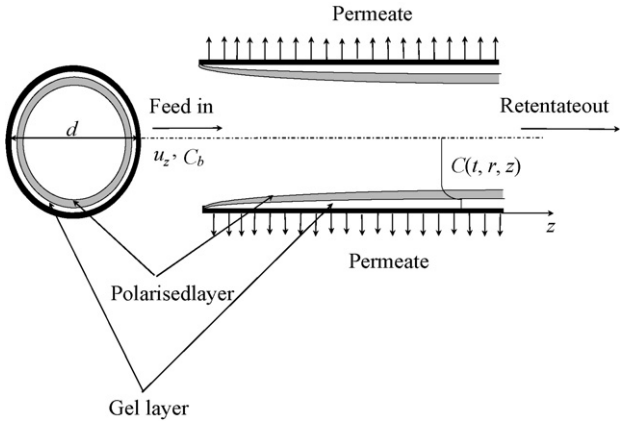

Fig. 2. Schematic diagram of tubular ultrafiltration process.

Before each run the membrane is cleaned using distilled water at 35 °C. This step was then followed by the determination of water flux. Recovery of the initial flux was possible, indicating that the fouled matters were easily removed, probably due to the high solubility of PEG in water.

3. Development of model

The conceptual representation of a tubular membrane ultrafiltration process is shown in Fig. 2 where the fluid that enters the membrane has a uniform concentration of solutes. Similarly at time zero, the solute concentration inside the tube is also uniform. It is assumed that the membrane is perfectly retentive and initially clean. Due to the pressure gradient across the membrane, the macromolecules of solute are driven towards the membrane wall but are too large to pass through it. As a result, a concentration polarization is developed above the membrane surface with solute concentration at the wall being higher then that in the bulk. At any time t from the beginning of the operation, the solute concentration in the tubular module is $C(t, r, z)$. The macromolecules would either remain as a stagnant gel layer on the membrane surface, or they may flow tangentially along it. Once a steady-state condition is reached, the stagnant solute layers at all positions along the membrane are at their maximum thickness. Consequently, the permeate flux would attain its steady-state value.

3.1. Convection–diffusion equation

The general mass balance equation:

$$\frac{D}{r}\frac{\partial}{\partial r}\left(r\frac{\partial C}{\partial r}\right) = u_r\frac{\partial C}{\partial r} + u_z\frac{\partial C}{\partial z} \quad (1)$$

The axial velocity of u_z can be obtained from mass balance and is given as:

$$u_z = -\frac{4u_{lim}}{d}z + u_0 \quad (2)$$

The radial velocity is given as:

$$u_r = -u_{lim} \quad (3)$$

where u_{lim} is the limiting permeate flux at the membrane surface.

Eq. (1) can be written in the dimensionless form by defining the following variables:

$$\phi = \frac{z}{L}, \eta = \frac{r}{d/2}$$

the equation becomes

$$\frac{\partial^2 C}{\partial \eta^2} + \left(\frac{1}{\eta} + \beta\right)\frac{\partial C}{\partial \eta} = \gamma \frac{\partial C}{\partial \phi} \quad (4)$$

where $\beta = du_{\lim}/2D$ and $\gamma = d^2 u_z/4DL$.

Eq. (4) can be solved numerically by using the following boundary conditions:

$$\phi = 0 \quad C(\eta, 0) = C_b$$

$$\eta = \delta_g \quad \frac{\partial C}{\partial \eta} + \beta C_g = 0$$

$$\eta = \delta_{gp} \quad C = C_b$$

where δ_g and δ_{gp} are the gel layer and the combined gel-polarized layer thickness, respectively.

3.2. Growth rate of gel layer

The presence of a gel layer on the membrane surface offers an additional resistance to the flow of permeate. On the assumption that the gel resistance, R_g, acts in series with R_m, the resulting permeate flux can be written as follows:

$$u_p = \frac{\Delta p}{R_m + \tilde{R}_g l} \quad (5)$$

The formation of a gel layer on the membrane surface in cross-flow ultrafiltration depends on the rate of particle deposition and the rate of particle re-entrainment into the bulk flow. By assuming that the gel formed is incompressible with a constant void fraction, and that no particles are present in the permeate, the net rate of gel formation is given by

$$\frac{dl}{dt} = \frac{u_p \bar{\varepsilon}}{\varepsilon_g - \bar{\varepsilon}} - f_1(u_z, \bar{\varepsilon}) f_2(\Delta p) \quad (6)$$

The solidosity, ε, can be evaluated from the solute concentration, C(wt.%), and the solute and the solvent densities by the relationship:

$$\varepsilon = \frac{0.01 R_d C}{1 + 0.01 C(R_d - 1)} \quad (7)$$

where R_d is the ratio of solute to solvent density. The solidosity of gel, ε_g, is assumed to be constant and independent of operating conditions. Its value can be estimated by substituting the appropriate value of C_g in the above equation. C_g can be obtained from the intercept of the plot of steady-state permeate flux, $u_{p,st}$, versus $\ln C_b$.

The first term on the right hand side of Eq. (6) represents the rate of particle deposition, which can be obtained through mass balance under static condition. The second term is the rate of particle re-entrainment and is a function of cross-flow velocity as supported by many experimental observations.

Under steady-state conditions, i.e. the rate of particle deposition is equal to the rate of re-entrainment, from experimental observations, it has been found that the steady-state permeate flux $u_{p,st}$ varies linearly with $\sqrt{u_0}$ (at a given C_b and Δp). The dependency of $u_{p,st}$ on C_b is taken to be directly proportional to $\varepsilon_g - \bar{\varepsilon}_{st}$. Limiting flux represents the maximum stationary permeation flux which can be reached when increasing transmembrane pressure. Hence, the limiting flux can be obtained when making transmembrane pressure large enough i.e. $f_2(\Delta p)$ = constant.

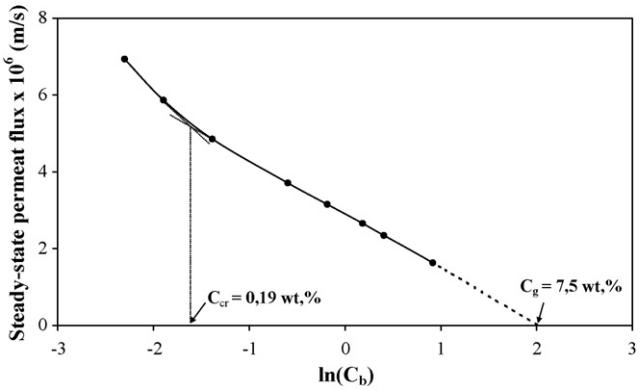

Fig. 3. Plot of steady-state permeate flux versus $\ln(C_b)$ at TMP = 4.7 bar, u_z = 0.15 m/s.

By combining the effects of the two parameters u_z and C_b, the limiting permeate flux can be expressed as:

$$u_{\lim} = A(\varepsilon_g - \bar{\varepsilon}_{st})\sqrt{u_0} \quad (8)$$

where $\bar{\varepsilon}_{st}$ is the steady-state value of the average solidosity in the polarized layer. The constant A depends on the solute-membrane system.

4. Numerical solution

Eq. (4) was rewritten in the finite difference using implicit scheme. Detailed derivation of the finite difference equation is given in Appendix A. The obtained equations form a tridiagonal system which was solved using TDMA algorithm. The value of ε_g = 0.108 used in the numerical simulation was estimated from Eq. (7) based on the value of C_g. The diffusivity of the polyethylene glycol was taken equal to 8×10^{-11} m^2/s. The iterative procedure is as following:

a. Starting with a initial value of $u_{\lim} = 0$.
b. Resolving the discretised equations given in the appendix by using TDMA algorithm.
c. Calculating $\varepsilon_{i,j}$ by using Eq. (7).
d. Calculating the average solidosity in the polarized layer, $\bar{\varepsilon}_{st} = \left(\sum_{j=0}^{m}\sum_{i=0}^{n}\varepsilon_{i,j}\right)/n \times m$, where n and m are the number of points of discretization in the radial and axial directions, respectively.
e. Calculating the new value of $u_{\lim}$ by using Eq. (8).
f. Continue from step (b) if the following condition is not satisfied, $\left|\frac{u_{\lim,prev} - u_{\lim,new}}{u_{\lim,new}}\right| < epsilon$.

5. Results and discussion

5.1. Determination of C_g

By measuring the steady-state permeate flux rates at several values of C_b, the results are plotted semi-logarithmically and a straight line is drawn through the data points (Fig. 3). This line is extended to the point of zero steady-state permeate flux where the corresponding value of C_b is taken to equal 7.5%.

5.2. Determination of the constant A

The value of the constant A was estimated from Eq. (8). In this estimation, $\bar{\varepsilon}_{st}$ was substituted with the bulk solidosity, ε_b. The validity of using ε_b instead of $\bar{\varepsilon}_{st}$ will be discussed later. For a given condition, a plot of $u_{\lim}$ versus $\sqrt{u_z}$ would yield a linear relationship with the slope equals to $A(\varepsilon_g - \bar{\varepsilon}_{st})$. Such plot

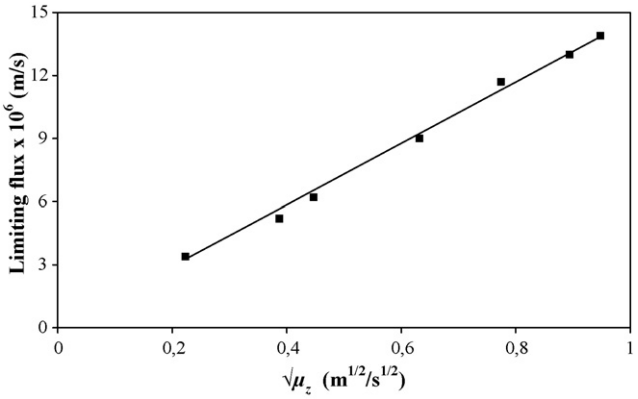

Fig. 4. Plot of steady-state permeate flux versus $\sqrt{u_z}$ at C_b = 0.25 wt.% and TMP = 1.7 bar.

for C_b = 0.25 wt.% is shown in Fig. 4. Similar dependence of u_{lim} behaviour on u_z was reported by some researchers [7–9]. The values of ε_g = 0.108 and $\bar{\varepsilon}_{st} = 0.0037$ were estimated from Eq. (7) based on the values of C_g = 7.5 wt.% and C_b = 0.25 wt.%. From the slope of 1.46×10^{-5} m$^{1/2}$/s$^{1/2}$, A was found to be equal 1.4×10^{-4} m$^{1/2}$/s$^{1/2}$.

5.3. Model prediction

Fig. 5 shows the experimental and predicted limiting flux. The data presented in Fig. 5 were obtained at u_z = 0.2 m/s for different bulk concentrations. As shown, the model can accurately predict the limiting flux. The validity of the model is further supported by the plot given in Fig. 6. The data presented in Fig. 6 are different from that used in the determination of the constant A.

Most of the existing models that considered the formation of a gel layer ignored the existence of the polarized layer above it. With this assumption, the solidosity of the liquid at the gel–liquid interface must necessarily be equal to the bulk solidosity. To assess the errors generated as a result of this assumption, a comparison is made by comparing the values of the average solidosity in the polarized layer generated by the present model to the bulk solidosity values. The Table 1 presents the simulated average solidosity in the polarized layer together with the bulk solidosity. It can be observed that the average solidosity is always greater than the bulk solidosity. It increases with increasing the bulk concentration. The bulk concentration of 0.25 wt.% is close to 0.19 wt.% concentration at which the two straight lines on the plot of $u_{p,st}$ versus ln(C_b) crossed each other as shown in Fig. 3. It is more probable that at concentrations below this critical value, the gel layer that formed on the membrane surface may not fully developed. For bulk concentrations near the critical concentration, the concentration polarization has no effect on limiting flux. Its effect is more pronounced when increasing C_b beyond the critical concentration. The result of this analysis clearly justify the use of bulk solidosity in Eq. (8) to estimate the empirical constant A.

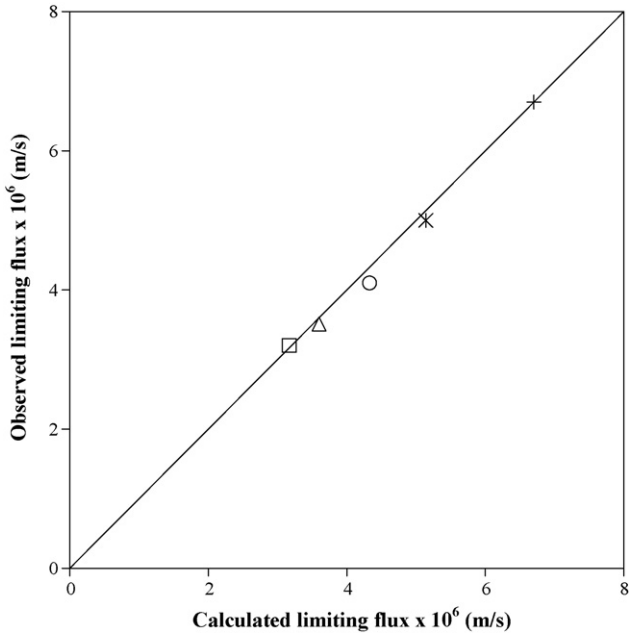

Fig. 5. Observed limiting flux versus calculated limiting flux at u_z = 0.2 m/s for different bulk concentrations +: 0.25 wt.%; *: 0.55 wt.%; ○: 0.83 wt.%; △: 1.2 wt.%; □: 1.5 wt.%.

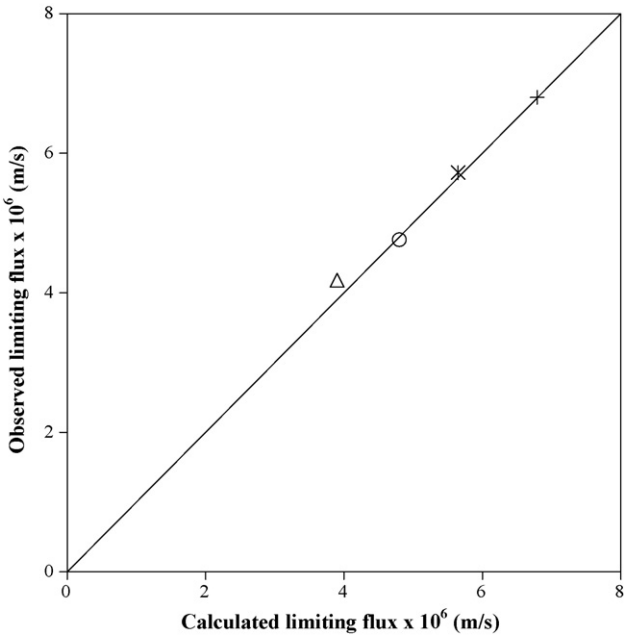

Fig. 6. Observed limiting flux versus calculated limiting flux at u_z = 0.35 m/s for different bulk concentrations +: 0.55 wt.%; *: 0.83 wt.%; ○: 1.2 wt.%; △: 1.5 wt.%.

Table 1
Computed average solidosity in the polarized layer for different bulk concentrations.

Bulk concentration, C_b (wt.%)	Bulk solidosity, ε_b	Average solidosity, $\bar{\varepsilon}_{st}$
0.25	0.00374	0.00375
0.55	0.0082	0.0280
0.83	0.0103	0.0400
1.20	0.0179	0.0520
1.50	0.0223	0.0580

6. Conclusion

The present model which has been developed based on the formation of a gel layer and the existence of a polarized layer above the gel, gave a satisfactorily prediction of the limiting flux during tubular ultrafiltration of PEG. Beyond the critical concentration, both concentration polarization and gel formation are the main factors controlling limiting flux in the tubular UF system. The effect of concentration polarization on limiting flux was found to be function of bulk concentration. It increases with increasing bulk concentration.

Appendix A.

Finite difference equations for Eq. (4) based on implicit scheme. Theses equations are as follows:

$$\frac{\partial^2 C}{\partial \eta^2} = \frac{C_{i+1}^{j+1} - 2C_i^{j+1} + C_{i-1}^{j+1}}{2\Delta\eta} \tag{A.1}$$

$$\frac{\partial C}{\partial \eta} = \frac{C_{i+1}^{j+1} - C_{i-1}^{j+1}}{2\Delta\eta} \tag{A.2}$$

$$\frac{\partial C}{\partial \Phi} = \frac{C_i^{j+1} - C_i^{j}}{\Delta\Phi} \tag{A.3}$$

By substituting Eqs. (A.1)–(A.3) into Eq. (4) we get

$$c_i C_{i+1}^{j+1} + a_i C_{i-1}^{j+1} + b_i C_i^{j+1} = C_i^j \tag{A.4}$$

where

$$c_i = -\left(s + \frac{s}{2i} + \frac{\beta s \Delta\eta}{2}\right)$$

$$a_i = -s + \frac{s}{2i} + \frac{\beta s \Delta\eta}{2}$$

$$b_i = (1 + 2s)$$

$$\beta = du_{\lim}/2D$$

$$s = \Delta\Phi/(\gamma\Delta\eta^2)$$

$$\gamma = (d^2 u_z)/(4DL)$$

$$\text{for } i = 2 \qquad c_2 C_3^{j+1} + b_2 C_2^{j+1} = C_2^j - a_2 C_1^{j+1} \tag{A.5}$$

$$\text{for } i = 3 \text{ to } n-2 \qquad c_i C_{i+1}^{j+1} + a_i C_{i-1}^{j+1} + b_i C_i^{j+1} = C_i^j \tag{A.6}$$

$$\text{for } i = n-1 \qquad a_{n-1} C_{n-2}^{j+1} + b_{n-1} C_{n-1}^{j+1} = C_{n-1}^j - c_{n-1} C_n^{j+1} \tag{A.7}$$

Eqs. (A.5)–(A.7) from a tridiagonal system that can be solved together with the boundary conditions by using TDMA algorithm.

References

[1] G. Jonsson, Transport phenomena in ultrafiltration: membrane selectivity and boundary layer phenomena, Pure Appl. Chem. 58 (1986) 1647–1656.
[2] A.S. Grandison, W. Youravong, M.J. Lewis, Hydrodynamic factors affecting flux and fouling during ultrafiltration of a skimmed milk, LAIT 80 (2000) 165–174.
[3] P. Bacchin, A possible link between critical and limiting flux for colloidal systems: consideration of critical deposit formation along a membrane, J. Membr. Sci. 228 (2004) 237–241.
[4] M.C. Porter, Concentration polarization with membrane ultrafiltration, Ind. Eng. Chem. Prod. Res. Develop. 11 (1972) 234–248.
[5] D.R. Trettin, M.R. Doshi, Limiting flux in ultrafiltration of macromolecular solutions, Chem. Eng. Commun. 4 (1980) 507–522.
[6] P. Aimar, R. Field, Limiting flux in membrane separation: a model based on the viscosity dependency of the mass transfer, Chem. Eng. Sci. 47 (1992) 579–586.
[7] A. Beicha, R. Zaamouche, N.M. Sulaiman, Dynamic ultrafiltration model based on concentration polarization-cake layer interplay, Desalination 242 (2009) 138–148.
[8] M.Z. Sulaiman, N.M. Sulaiman, A. Beicha, Prediction of dynamic permeate flux during cross-flow ultrafiltration of polyethylene glycol using concentration polarization-gel layer model, J. Membr. Sci. 189 (2001) 151–165.
[9] N. Ghaffour, Modelling of fouling phenomena in cross-flow ultrafiltration of suspensions containing suspended solids and oil droplets, Desalination 167 (2004) 281–291.